inter.noise
HAMBURG 2016

Modelling vibration transmission on frameworks of beams using Advanced Statistical Energy Analysis

Carl HOPKINS[1]; Xing WANG[1,2]

[1] Acoustics Research Unit, University of Liverpool, Liverpool, UK

[2] National Key Laboratory of Science and Technology on Vessel Integrated Power System, Navy University of Engineering, P.R. China

ABSTRACT

To account for indirect coupling and high propagation losses on frameworks of coupled beams, Advanced Statistical Energy Analysis (ASEA) has been used to study bending and torsional wave models, and bending and longitudinal wave models on frameworks of beams. At high-frequencies, Timoshenko theory was incorporated into ASEA by changing the group velocity used to calculate the coupling loss factors, but maintaining the Euler-Bernoulli beam transmission coefficients. Comparisons of FEM, SEA and ASEA show that high propagation losses can occur with a rectangular beam frame, while tunneling exists in a three-bay linear grillage which has relatively short beam lengths. Unlike SEA, ASEA is shown to be able to account for the indirect coupling and these losses. For a three-bay linear grillage, comparisons with FEM show that ASEA is able to predict the response on the 'perfectly periodic' structure as well as a more realistic engineering structure with uncertainty in the Young's modulus.

Keywords: vibration, beams I-INCE Classification of Subjects Number(s): 43.2, 75.2

1. INTRODUCTION

Frameworks of beams are often employed in engineering structures for marine, aeronautic, automotive and building applications for which prediction models are needed to estimate vibration transmission for noise and vibration control.

This paper considers mid- and high-frequency prediction models based on classical Statistical Energy Analysis (SEA) (1) and Advanced SEA (ASEA) (2) for frameworks of beams with multiple wave types up to high frequencies where Timoshenko beam theory is valid. With systems of coupled beams, the validation of statistical models must consider the following combination of factors: low mode counts, low modal overlap, multiple wave types, different bending wave theories, propagation losses and indirect coupling as well as increasing uncertainty in measurements at high frequencies. Hence SEA and ASEA are not only compared with each other, but with Finite Element Methods (FEM) and measurements.

Heron (2) developed ASEA which combines SEA with ray tracing ignoring phase effects to track the power transmitted between coupled subsystems. This approach was validated with excitation of longitudinal waves at one end of an in-line array of six rods. Subsequently Yin and Hopkins (3,4) used ASEA to predict bending wave transmission across two coupled plates where one plate was a periodic ribbed plate at high frequencies where each bay supported local modes and could be modelled as a separate subsystem. It was shown that indirect coupling between bays at high-frequencies was sufficiently dominant that SEA underestimated the response by ≈40dB on the furthest bay whereas ASEA gave close agreement with measurements and FEM. This was because ASEA accounted for spatial filtering due to transmission across each rib that led to non-diffuse vibration fields on the most distant bays. Wilson and Hopkins (5) extended the application of ASEA to large structures built from many coupled plates by introducing beam tracing to increase computational efficiency. This allowed modelling of large periodic box-like structures for which spatial filtering of bending waves becomes apparent in the low- and mid-frequency ranges after only a few structural junctions. The inclusion of

[1] carl.hopkins@liverpool.ac.uk
[2] xingwang.v@qq.com

indirect coupling in ASEA provided significantly better estimates than SEA when plates had at least one or two bending modes in each one-third octave band, although the modal overlap was relatively high due to significant coupling losses. This paper considers the application of ASEA to beams over a wide frequency range. In the high-frequency range, Timoshenko bending theory is applicable and propagation losses are expected to become increasingly important due to lower group velocities than Euler-Bernoulli theory. However, validated methodologies concerning the changeover from Euler-Bernoulli to Timoshenko bending theory using SEA and ASEA are absent from the literature.

2. CLASSICAL SEA AND ADVANCED SEA

2.1 SEA

The SEA matrix solution is given by

$$\begin{bmatrix} \sum_{n=1}^{N}\eta_{1n} & -\eta_{21} & -\eta_{31} & \cdots & -\eta_{N1} \\ -\eta_{12} & \sum_{n=1}^{N}\eta_{2n} & -\eta_{32} & \cdots & -\eta_{N2} \\ -\eta_{13} & -\eta_{23} & \sum_{n=1}^{N}\eta_{3n} & \cdots & -\eta_{N3} \\ \vdots & \vdots & \vdots & \ddots & \vdots \\ -\eta_{1N} & -\eta_{2N} & -\eta_{3N} & \cdots & \sum_{n=1}^{N}\eta_{Nn} \end{bmatrix} \begin{bmatrix} E_1 \\ E_2 \\ E_3 \\ \vdots \\ E_N \end{bmatrix} = \begin{bmatrix} \frac{W_{\mathrm{in}(1)}}{\omega} \\ \frac{W_{\mathrm{in}(2)}}{\omega} \\ \frac{W_{\mathrm{in}(3)}}{\omega} \\ \vdots \\ \frac{W_{\mathrm{in}(N)}}{\omega} \end{bmatrix} \tag{1}$$

where $W_{\mathrm{in}(i)}$ is the power input into source subsystem i, ω is the band centre angular frequency, E_i is the time and space average energy of subsystem i, η_{ii} is the Internal Loss Factor (ILF) of subsystem i, η_{ij} is the Coupling Loss Factor (CLF) from subsystem i to j.

2.2 Advanced SEA

ASEA was introduced by Heron (2) and considers the available power per unit modal energy and the unavailable power per unit modal energy. This allows unavailable power to be defined as power lost due to propagation across a subsystem.

Available power corresponds to stored modal energy which is the only form of energy that is considered in SEA. The link between ASEA and SEA can be seen by rewriting Eq. **Error! Reference source not found.** in the form, $\mathbf{A}_0\mathbf{e}_0+\mathbf{M}\mathbf{e}_0=\mathbf{P}_0$, in which $\mathbf{M}=\mathrm{diag}\{\omega n_\mathrm{i}\eta_\mathrm{ii}\}$ is a diagonal matrix of modal overlap factors, the total modal energy matrix is $\mathbf{e}_0=[E_1/n_1, E_2/n_2, \ldots, E_\mathrm{N}/n_\mathrm{N}]$, n_i is the modal density of subsystem i, $\mathbf{P}_0$ is the column vector of input powers, and $\mathbf{A}_0$ is defined as

$$\mathrm{A}_0 = \omega \begin{bmatrix} \sum_{k\neq 1}^{N} n_1\eta_{1\mathrm{k}} & -n_2\eta_{21} & \cdots & -n_N\eta_{N1} \\ -n_1\eta_{12} & \sum_{k\neq 2}^{N} n_2\eta_{2\mathrm{k}} & \cdots & -n_N\eta_{N2} \\ \vdots & \vdots & \ddots & \vdots \\ -n_1\eta_{1N} & -n_2\eta_{2N} & \cdots & \sum_{k\neq N}^{N} n_N\eta_{N\mathrm{k}} \end{bmatrix} \tag{2}$$

ASEA requires solution of the following two equations:

$$\mathbf{P} = \mathbf{Ae} + \mathbf{Me} \tag{3}$$

$$\mathbf{Q} = \mathbf{Be} + \mathbf{Md} \tag{4}$$

where P and Q are the available and unavailable power input vectors respectively. The available modal energy is denoted by **e** and unavailable modal energy is denoted by **d**; hence **Me** and **Md** give the available power lost and unavailable power lost within each subsystem respectively. Matrix **A** represents the power transfer from available power in a particular subsystem to available power in another subsystem (including that subsystem itself) whereas matrix **B** represents the transfer of available power to unavailable power. The number of times that the initial power is tracked across the source subsystem is defined as the ASEA level number. When the level number is zero there is no

transfer from available power to unavailable power and use of $\mathbf{A}_0$ with ASEA gives a result that is equivalent to SEA. In this paper the beams are excited with rain-on-the-roof; hence all the input power is available for transmission, so it can be treated as available power input in **P** whereas the unavailable power input in matrix **Q** is zero. The subsystem response is given by the total modal energy **e**+**d**.

2.3 Wave theory

For junctions of beams the coupling loss factor is calculated using

$$\eta_{ij} = \frac{c_{g,i}\tau_{ij}}{4\pi f L_i} \tag{5}$$

where $c_{g,i}$ is the group velocity of subsystem i, τ_{ij} is the transmission coefficient from subsystem i to subsystem j, and L_i is the beam length of subsystem i.

To cover bending wave vibration over a wide frequency range, one possibility would be to change over from Euler-Bernoulli to Timoshenko phase velocity when the difference between them is 10% because this percentage is currently used to define the thin beam limit. However, this is an arbitrary definition. Therefore as the coupling loss factor is proportional to the group velocity it is proposed to switch between Euler-Bernoulli to Timoshenko group velocities when there is at least a 1dB difference in the resulting coupling loss factor which corresponds to a 26% change in the group velocity. This is a more practical choice because it is unrealistic to expect the agreement between SEA or ASEA and the actual response of a single, large structure to be consistently less than 1dB.

For coupled beams that form a two-dimensional junction, four possible incident waves can be considered: Type A bending waves (defined here as having displacement in the same plane as the junction), Type B bending waves (defined here as having displacement perpendicular to the plane of the junction), longitudinal waves and torsional waves. For beams that are perpendicular to each other at the junction, excitation of Type A bending waves generates longitudinal waves, and excitation of Type B bending waves generates torsional waves at the junction.

For practical purposes the approach proposed in this paper is to determine transmission coefficients for insertion in Eq.(5) based on Euler-Bernoulli theory but switch from Euler-Bernoulli to Timoshenko group velocities when there is at least a 1dB difference in the resulting coupling loss factor which corresponds to a 26% change in the group velocity.

3. FINITE ELEMENT METHODS

Finite element calculations are carried out using Abaqus/CAE 6.12 with rain-on-the-roof excitation applied to each beam. Excitation of bending or longitudinal waves is applied using unity forces with random phase at each unconstrained node along the length of the beam. For excitation of torsional waves, this is applied by using unity moments with random phase. Ten sets of rain-on-the-roof are used and the results processed to calculate a mean value with 95% confidence intervals. FEM models are built with Euler-Bernoulli beam element B33 and Timoshenko beam element B31 for comparison with SEA and ASEA which implement Euler-Bernoulli or Timoshenko theory.

4. BEAM CONSTRUCTIONS

Two different frameworks of beams were used for modelling and also fabricated for laboratory measurements. These were a rectangular beam frame and a three-bay grillage. All beams are formed from Perspex for with a cross-section of 0.02m x 0.01m. For the rectangular beam frame (Figure 1(a)) the beam lengths are 1.3m and 1.0m whereas for the three-bay linear grillage (Figure 1(b) the beams are either 0.40m or 0.45m long (i.e. approximately half the length of the beams in the rectangular beam frame), in order to (a) reduce propagation losses, (b) increase the likelihood of indirect coupling and (c) allow measurable velocity levels on the furthest beam.

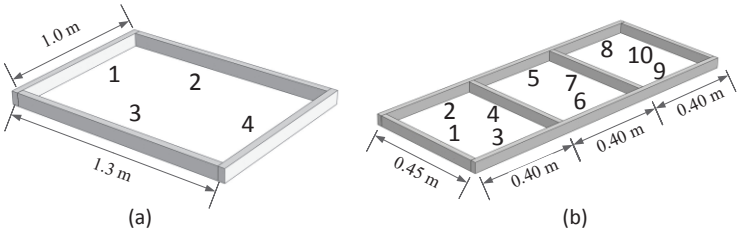

Figure 1 – (a) Rectangular beam frame, (b) Three-bay linear grillage

5. RESULTS

5.1 Rectangular beam frame

For the rectangular beam frame, results are shown with excitation of Type A bending waves on beam 1 for receiving subsystems representing bending wave energy in Figure 2(a,b) and for receiving subsystems representing longitudinal wave energy in Figure 2(c,d).

On Figure 2(a), measurements above 2kHz show closest agreement with FEM, SEA and ASEA using Euler-Bernoulli theory for transmission to bending wave motion on beam 2 which is directly connected to beam 1. However, for transmission to bending wave motion on beam 4 (which is not physically connected to the source beam) the results in Figure 2(b) indicate that FEM with either Euler-Bernoulli or Timoshenko elements agree closely with measurements.

For E_{B1}/E_{L2} on Figure 2(c) the confidence intervals from FEM using Euler-Bernoulli and Timoshenko elements overlap up to 20kHz and both show closest agreement with SEA or ASEA using Euler-Bernoulli group velocity. Above 2kHz for E_{B1}/E_{L4} on Figure 2(d) there is clear evidence that FEM with Euler-Bernoulli elements shows closest agreement with ASEA using Euler-Bernoulli group velocity, and FEM with Timoshenko elements shows closest agreement with ASEA using Timoshenko group velocity. At 20kHz the difference between Euler-Bernoulli and Timoshenko models is ≈7dB for both FEM and ASEA. The fact that ASEA shows close agreement with FEM using Timoshenko elements and that the energy level differences with ASEA are higher than SEA confirms the presence of significant propagation losses because this mechanism is included in ASEA, but not in SEA. It also confirms the assumption in ASEA that phase effects can be ignored.

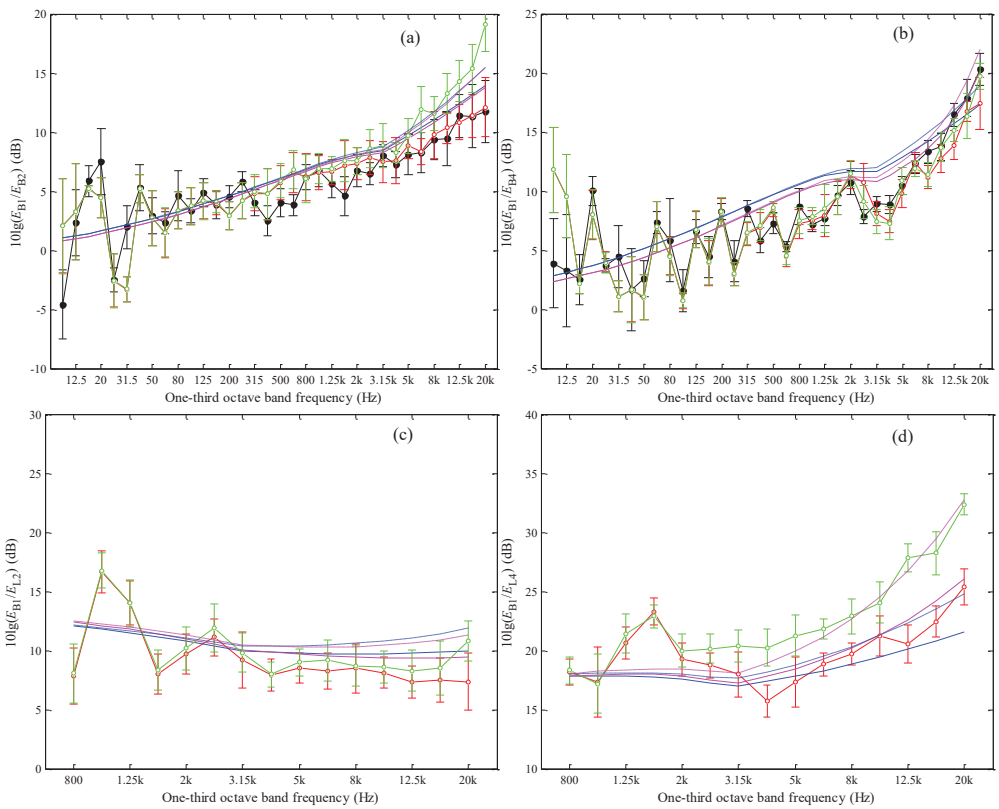

Figure 2 – Rectangular beam frame - Comparison of FEM, SEA (BL model) and ASEA (BL model) with excitation of Type A bending waves on subsystem B1. Receiving subsystems: (a) B2 (b) B4 (c) L2 (d) L4. —●—, Measurement; —○—, FEM (Euler-Bernoulli elements); —○—, FEM (Timoshenko elements); ———, SEA (Euler-Bernoulli group velocity); – – – –, SEA (Timoshenko group velocity); ———, ASEA (Euler-Bernoulli group velocity); – – – –, ASEA (Timoshenko group velocity). Results from measurements and FEM are shown with with 95% confidence intervals.

For the rectangular beam frame, results are shown with excitation of Type B bending waves on beam 1 for receiving subsystems representing bending wave energy in Figure 3(a,b) and for receiving subsystems representing torsional wave energy in Figure 3(c,d). For E_{B1}/E_{B4} between 315Hz and 2kHz, FEM using Euler-Bernoulli and Timoshenko elements are similar, and the difference compared with measurements is between 0.2dB and 2.2dB. However, for E_{B1}/E_{B4} above 2kHz it is clear that there is closest agreement with FEM using Timoshenko elements; this is evident near the peak in the energy level difference at 4kHz. Above 2kHz, FEM using Euler-Bernoulli elements follows the general trends of SEA or ASEA using Euler-Bernoulli group velocity. For E_{B1}/E_{B4} above 6.3kHz, FEM using Timoshenko elements closely follows ASEA using Timoshenko group velocity. This agreement, and the fact that ASEA has significantly higher energy level differences than SEA, indicates that ASEA correctly incorporates these high propagation losses.

Assessment of the conversion from bending waves on the source subsystem to torsional waves on a receiving subsystem is feasible above 2kHz as there are at least two bending and two torsional modes in each frequency band (modal overlap factor is at least 0.2 for both bending and two torsional waves) and the FEM curves become relatively smooth. For E_{B1}/E_{T2} and E_{B1}/E_{T4} between 2kHz and 20kHz, FEM using Euler-Bernoulli elements follows the general trends of SEA or ASEA using Euler-Bernoulli group velocity, and FEM using Timoshenko elements closely follows ASEA using Timoshenko group velocity. Again, this confirms the assumption in ASEA that phase effects can be ignored. The transmission coefficients from bending waves on one beam to torsional waves on the other beam are highest above 6.3kHz. Hence the combination of high propagation losses with Timoshenko group velocity and wave conversion at each junction results in high energy level differences (e.g. 34dB for E_{B1}/E_{B4} at 20kHz predicted using ASEA and FEM using Timoshenko elements).

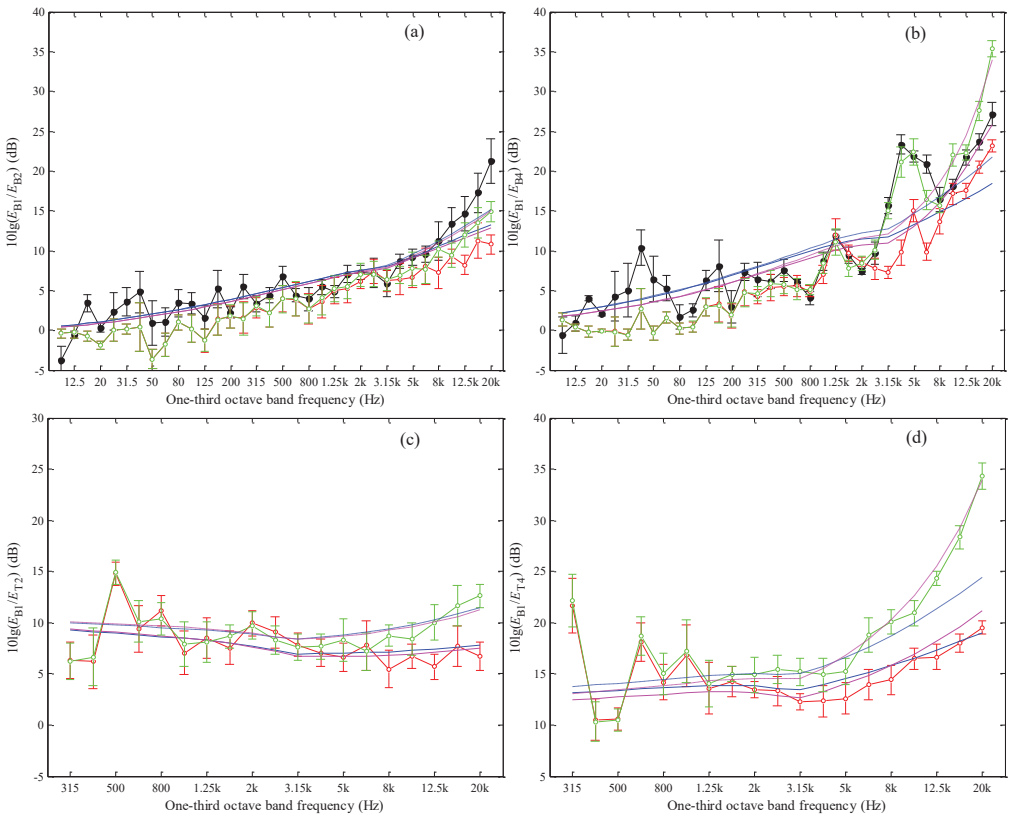

Figure 3 – Rectangular beam frame - Comparison of FEM, SEA (BT model) and ASEA (BT model) with excitation of Type B bending waves on subsystem B1. Receiving subsystems: (a) B2 (b) B4 (c) T2 (d) T4.

5.2 Three-bay linear grillage

Figure 4(a,b) compares measured and predicted energy level differences for the BL model where Type A bending waves are excited on the source beam 1, and the source and receiving subsystems represent Type A bending wave energy. There is close agreement between the average values from measurements, FEM (Euler-Bernoulli and Timoshenko elements) and ASEA (Euler-Bernoulli and Timoshenko group velocity). With increasing frequency, the generation of longitudinal waves at the junction typically increases the indirect coupling such that ASEA gives lower energy level differences than SEA as the beams become more distant from the source. However, the largest differences between SEA and ASEA do not always occur in the highest frequency band. In general, measurements and FEM show closest agreement with ASEA rather than SEA due to the existence of indirect coupling.

Figure 4(c,d) shows predicted energy level differences for the BL model where Type A bending waves are excited on the source beam 1 and the receiving subsystem represents longitudinal wave energy. These results show similarly close agreement between FEM and ASEA when both the source and receiving subsystems contain bending wave energy. The main finding here is that ASEA provides a better estimate of vibration transmission than SEA.

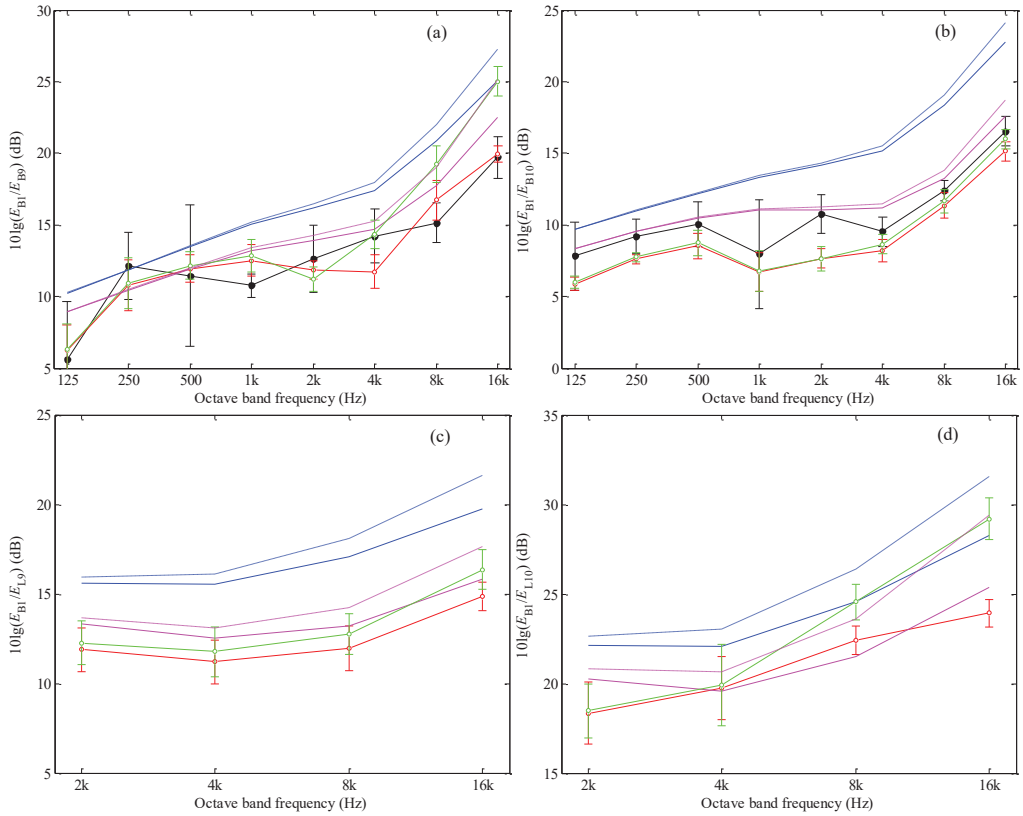

Figure 4 – Three-bay linear grillage frame - Comparison of FEM, SEA (BL model) and ASEA (BL model) with excitation of Type A bending waves on subsystem B1. Receiving subsystems: (a) B9 (b) B10 (c) L9 (d) L10.

For the BT model, Figure 5(a,b) allow comparison of measured and predicted energy level differences for Type B bending wave excitation where both source and receiving subsystems represent Type B bending wave energy. For the most distant subsystems 9 and 10, SEA overestimates the energy level difference by ≈4dB and there is closer agreement between measurements, FEM and ASEA (≈3.4dB difference) which also have overlapping 95% confidence intervals. Between 1kHz and 16kHz there are both bending and torsional modes. Measurements tend to show closest agreement with FEM using Timoshenko rather than Euler-Bernoulli theory. Differences between these FEM models becomes apparent at and above 4kHz although the difference between Timoshenko and Euler-Bernoulli group velocities is only ≥26%, at and above 8kHz. In general, ASEA with Timoshenko group velocity shows closest agreement with measurements and FEM using Timoshenko theory.

Figure 5(c,d) allows comparison of predicted energy level differences for the BT model where Type B bending waves are excited on the source subsystem and the receiving subsystem represents torsional wave energy. In general, FEM using Euler-Bernoulli elements shows closest agreement with ASEA using Euler-Bernoulli group velocity, and FEM using Timoshenko elements shows closest agreement with ASEA using Timoshenko group velocity.

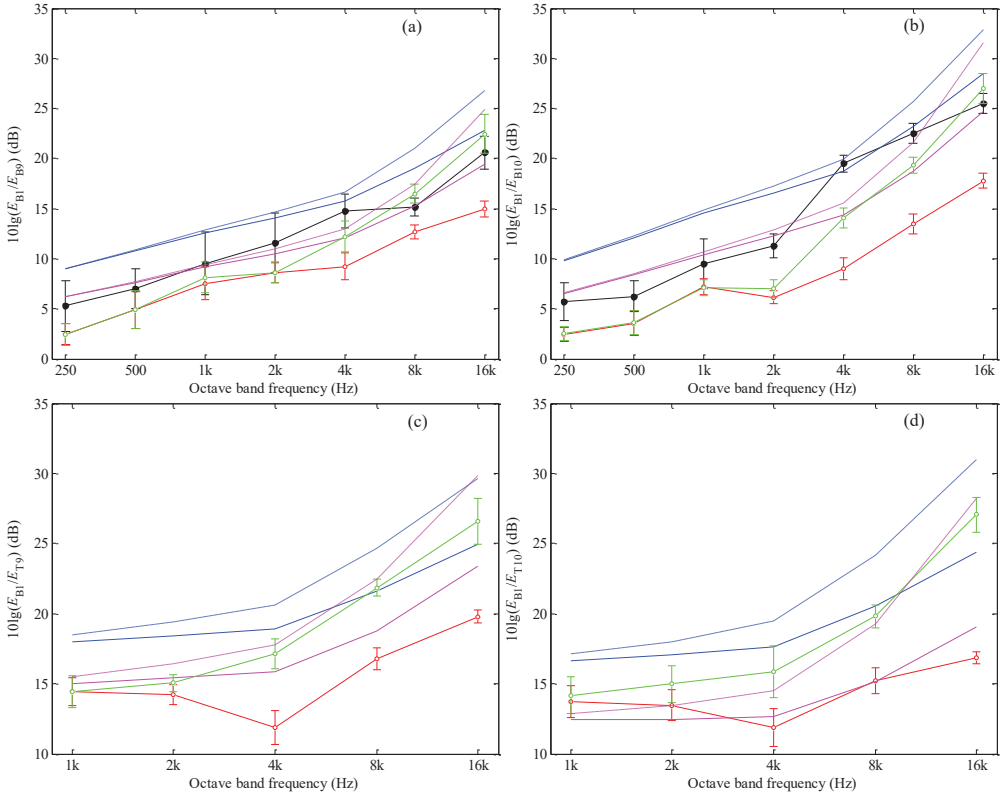

Figure 5 – Three-bay linear grillage frame - Comparison of FEM, SEA (BT model) and ASEA (BT model) with excitation of Type B bending waves on subsystem B1. Receiving subsystems: (a) B9 (b) B10 (c) T9 (d) T10.

5.2.1 Effect of uncertainty in the Young's modulus

To assess the effect of uncertainty in the material properties, a Monte Carlo simulation is carried out using FEM. An ensemble of ten different models of the three-bay linear grillage is created in which the Young's modulus for each beam in each grillage is determined by random sampling of values from a normal distribution based upon the mean and standard deviation from the measured Young's modulus for Perspex. For these data, the coefficient of variation (σ/μ) is 0.11.

It was noted that with longitudinal excitation there were a few level differences with discrepancies up to 5dB between ASEA and FEM for the perfectly periodic grillage. Figure 6 allows comparison of ASEA with FEM using uniform material properties and FEM with random Young's modulus. This shows closer agreement is obtained between ASEA and FEM with random Young's modulus because this ensures that the local modes of the beams that form the grillage are no longer identical.

Figure 7 shows the differences between the energy level differences predicted using FEM and those from ASEA for the BL model. The results indicate that regardless of whether Euler-Bernoulli or Timoshenko theory is used, the effect of uncertainty in the Young's modulus is to reduce the differences between FEM and ASEA to less than ≈3dB and to avoid a bias error where ASEA overestimates the energy level difference. This effect was more pronounced with excitation of longitudinal waves rather than excitation of bending or torsional waves; hence the BT model is not shown here.

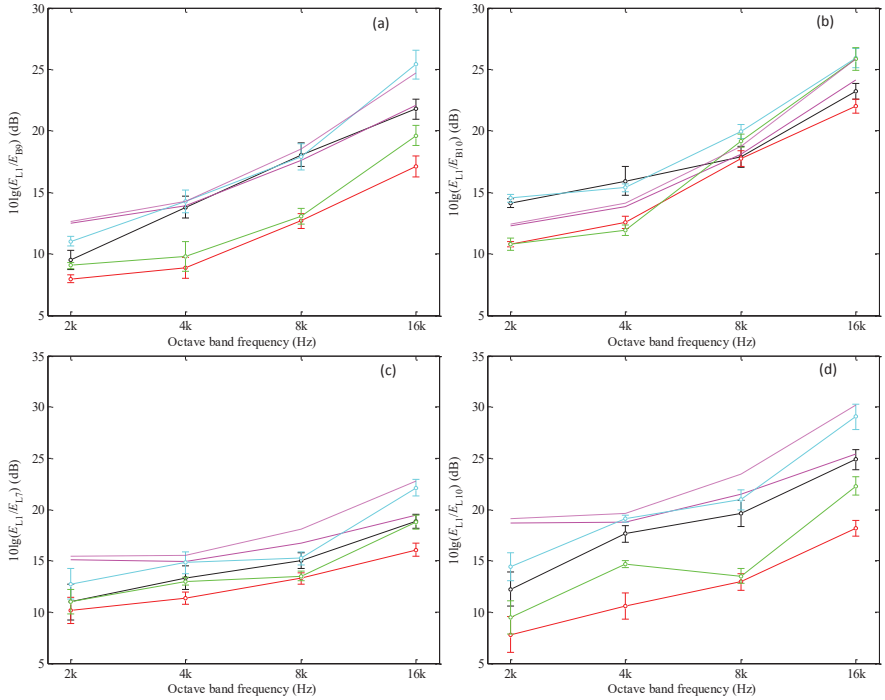

Figure 6 – BL model of longitudinal wave transmission on the three-bay grillage (Source subsystem: L1): comparison of FEM (uniform material properties), FEM (random Young's modulus) and ASEA. —o—, FEM (random Young's modulus) with Euler-Bernoulli elements; —o—, FEM (uniform material properties) with Euler-Bernoulli elements; —o—, FEM (random Young's modulus) with Timoshenko elements; —o—, FEM (uniform material properties) with Timoshenko elements; ———, ASEA (Euler-Bernoulli group velocity); – – – –, ASEA (Timoshenko group velocity). Results from FEM are shown with 95% confidence intervals.

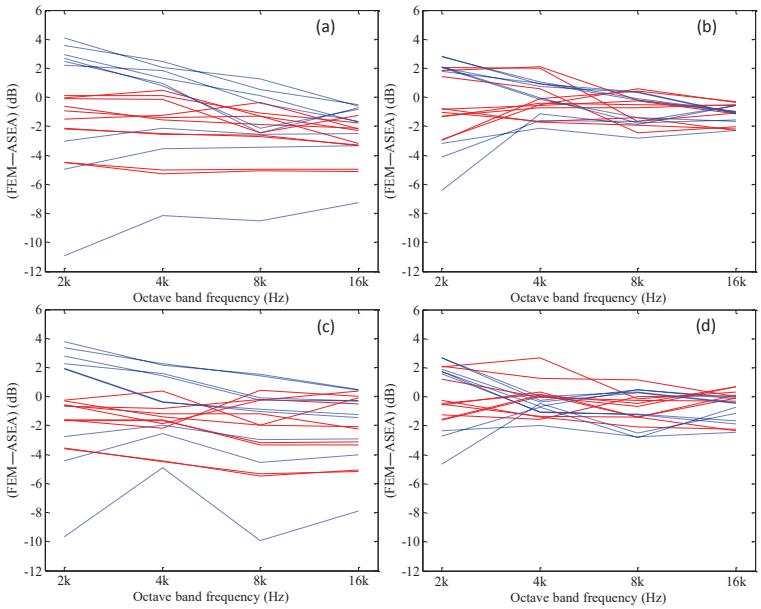

Figure 7 – Difference between FEM and ASEA energy level differences for BL model on the three-bay grillage (Source subsystem: L1): (a) FEM (uniform material properties) with Euler-Bernoulli elements, ASEA (Euler-Bernoulli group velocity); (b) FEM (random Young's modulus) with Euler-Bernoulli elements, ASEA (Euler-Bernoulli group velocity); (c) FEM (uniform material properties) with Timoshenko elements, ASEA (Timoshenko group velocity); (d) FEM (random Young's modulus) with Timoshenko elements, ASEA (Timoshenko group velocity). ———, bending receiving subsystem; – – – –, longitudinal receiving subsystem.

6. CONCLUSIONS

To assess the validity of ASEA with multiple wave types at high frequencies where Timoshenko bending theory is valid, coupling loss factors are calculated using wave theory transmission coefficients based on Euler-Bernoulli theory but using Timoshenko (rather than Euler-Bernoulli) group velocity. The proposal is to switch from Euler-Bernoulli to Timoshenko group velocities when there is at least a 1dB difference in the resulting coupling loss factor which corresponds to a 26% change in the group velocity. For beams with relatively high propagation losses, the agreement between ASEA and FEM indicates that (a) unlike SEA, ASEA is able to predict high propagation losses, (b) it is reasonable to ignore phase effects in the ray tracing approach used with ASEA, and (c) changing over from Euler-Bernoulli to Timoshenko theory in SEA and ASEA can be achieved by changing the group velocity used to calculate the coupling loss factors. However, when propagation losses are not significant because the beams are sufficiently short, indirect coupling (tunneling mechanisms) can become increasingly important. For rain-on-the-roof excitation of bending waves on a perfectly periodic, finite three-bay linear grillage there was reasonable agreement between measurements, FEM and ASEA. The differences between FEM and ASEA were less than ≈5dB and could be partly attributed to neglecting phase effects in ASEA. To investigate the more realistic situation of an imperfectly periodic, finite linear grillage, numerical experiments with FEM were used to introduce uncertainty into the Young's modulus for each beam that forms the linear grillage. Results show that for beams modelled with Euler-Bernoulli or Timoshenko theory, the effect of this uncertainty was to reduce all the differences between FEM and ASEA to less than ≈3dB.

ACKNOWLEDGEMENTS

Xing Wang is grateful for the PhD funding provided by the China Scholarship Council and the University of Liverpool.

REFERENCES

1. Lyon RH, DeJong RG. Theory and application of statistical energy analysis (Butterworth-Heinemann, MA, USA, 1995).
2. Heron KH. Advanced statistical energy analysis. Phil Trans R Soc Lond. 1994;A346:501-510.
3. Yin J, Hopkins C. Prediction of high-frequency vibration transmission across coupled, periodic ribbed plates by incorporating tunnelling mechanisms. J Acoust Soc Am. 2013;133(4):2069-2081.
4. Yin J, Hopkins C. Modelling bending wave transmission across coupled plate systems comprising periodic ribbed plates in the low-, mid-, and high-frequency ranges using forms of Statistical Energy Analysis. Shock and Vibration. 2015 Jan 1;501:467875.
5. Wilson D, Hopkins C. Analysis of bending wave transmission using beam tracing with advanced statistical energy analysis for periodic box-like structures affected by spatial filtering. J Sound Vib 2015:341: 138-161.